PROCEEDINGS OF SPIE

SPIEDigitalLibrary.org/conference-proceedings-of-spie

The MAORY laser guide star wavefront sensor: design status

Laura Schreiber, Philippe Feautrier, Eric Stadler, Patrick Rabou, Jean-Jacques Correia, et al.

Laura Schreiber, Philippe Feautrier, Eric Stadler, Patrick Rabou, Jean-Jacques Correia, Laurence Glück, Sylvain Rochat, Laurent Jocou, Yves Magnard, Thibaut Moulin, Alain Delboulbé, Sylvain Douté, Gaël Chauvin, Estelle Moraux, Sylvain Oberti, Christophe Verinaud, Fausto Cortecchia, Carmelo Arcidiacono, Emiliano Diolaiti, Paolo Ciliegi, Michele Bellazzini, Simone Esposito, Lorenzo Busoni, Roberto Ragazzoni, "The MAORY laser guide star wavefront sensor: design status," Proc. SPIE 10703, Adaptive Optics Systems VI, 107031Y (10 July 2018); doi: 10.1117/12.2314467

SPIE.

Event: SPIE Astronomical Telescopes + Instrumentation, 2018, Austin, Texas, United States

The MAORY Laser Guide Star Wavefront Sensor: Design status

Laura Schreiber[a], Philippe Feautrier[b], Eric Stadler[b], Patrick Rabou[b], Jean-Jacques Correia[b], Laurence Glück[b], Sylvain Rochat[b], Laurent Jocou[b], Yves Magnard[b], Thibaut Moulin[b], Alain Delboulbé[b], Sylvain Douté[b], Gaël Chauvin[b], Estelle Moraux[b], Sylvain Oberti[c], Christophe Verinaud[c], Fausto Cortecchia[a], Carmelo Arcidiacono[a], Emiliano Diolaiti[a], Paolo Ciliegi[a], Michele Bellazzini[a], Simone Esposito[d], Lorenzo Busoni[d], and Roberto Ragazzoni[e]

[a]INAF - Osservatorio di Astrofisica e Scienza dello Spazio di Bologna, Via Gobetti 93/3, 40129 Bologna, Italy
[b]Université Joseph Fourier-Grenoble 1/CNRS-INSU, Institut de Planétologie et d'Astrophysique de Grenoble (IPAG) UMR 5274, Grenoble, F-38041, France
[c]European Southern Observatory, Karl-Schwarzschild-Str. 2, D-85748 Garching b. Muenchen, Germany
[d]INAF - Osservatorio Astrofisico di Arcetri, largo E. Fermi 5, 50125 Firenze, Italy
[e]INAF - Osservatorio Astronomico di Padova, vicolo dell'Osservatorio 5, 35122 Padova, Italy

ABSTRACT

MAORY will be the multi-adaptive optics module feeding the high resolution camera and spectrograph MICADO at the Extremely Large Telescope (ELT) first light. In order to ensure high and homogeneous image quality over the MICADO field of view and high sky coverage, the baseline is to operate wavefront sensing using six Sodium Laser Guide Stars. The Laser Guide Star Wavefront Sensor (LGS WFS) is the MAORY sub-system devoted to real-time measurement of the high order wavefront distortions. In this paper we describe the MAORY LGS WFS current design, including opto-mechanics, trade-offs and possible future improvements.

Keywords: Extremely Large Telescope, Multi-Conjugate Adaptive Optics, Wavefront sensing, Laser Guide Stars

1. INTRODUCTION

MAORY[1] is the multi-adaptive optics module for the ELT[2] first light. It will provide a corrected Field-of-View of about 1 arcminute diameter to its client instrument MICADO,[3] a near-infrared camera and spectrograph. A second port will be available for a second instrument still to be determined. The MAORY consortium is composed mainly by Italian institutes part of the Italian National Institute of Astrophysics (INAF), with the exception of the Institut de Planétologie et d'Astrophysique de Grenoble (IPAG), that is responsible for the Laser Guide Star Wavefront-sensor sub-system. The European Southern Observatory is also involved in the development of the instrument. The MAORY baseline is to operate wavefront sensing by the means of six Laser Guide Stars and three Natural guide stars. The six Laser Guide Stars are used to sense the high orders at a frequency of about 500 Hz.[4] The infrared part of the three Natural Guide Stars light is used for the fast measurement of tip-tilt focus and astigmatisms,[5,6] while the visible part is used for truth sensing with a frame rate that can go from tens of Hz to 100 Hz, depending on the guide star magnitude.[7] These sensors should also see the spurious aberrations injected in the loop by the Laser Guide Star spot truncation effect and its variations.[8] The wavefront correction is operated by M4/M5,[9] that are part of the telescope, and by 2 post focal deformable mirrors.

Fig. 1 shows a schematic overview of the MAORY instrument with a simple block diagram. The light from the ELT is propagated through the MAORY common path optics.[10] Upon wavefront compensation by the Post-focal

Further author information: (Send correspondence to Laura Schreiber)
Laura Schreiber: E-mail: laura.schreiber@oabo.inaf.it

Adaptive Optics Systems VI, edited by Laird M. Close, Laura Schreiber, Dirk Schmidt, Proc. of SPIE Vol. 10703, 107031Y · © 2018 SPIE
CCC code: 0277-786X/18/$18 · doi: 10.1117/12.2314467

deformable mirrors, the light is split by a Dichroic beam-splitter: the light of wavelength shorter than about 600 nm is propagated to the LGS Path Optics and then to the LGS WFS sub-system. The longer wavelengths are reflected in the direction of MICADO on the top of which is mounted the NGS Wavefront-sensor MAORY sub-system. At this level the light is splitted in field: the central arcminute goes to the MICADO instrument while the external doughnut (up to 3 arcminutes diameter) is dedicated to the natural guide stars technical field. For each LGS WFS channel, a fast tip-tilt compensation of the Laser jitter at the laser launcher level, and a slower focus correction of the Sodium altitude variation are foreseen.

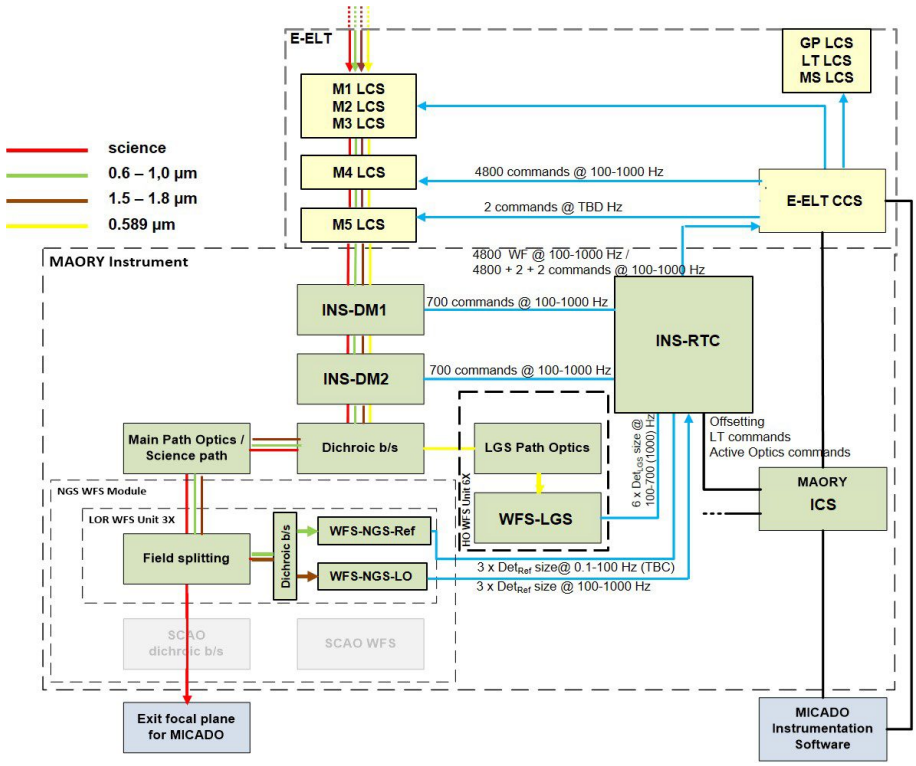

Figure 1. MAORY AO subsystem overview (MCAO configuration). Red lines: science light path. Yellow lines: LGS light path. Green lines: NGS visible light path. Brown lines: NGS infrared light path. Blue lines: real-time signals. Black lines: non real-time signals. Blocks in light grey are not used in MCAO mode. Those devices inside the E-ELT dashed box (yellow boxes) do not belong to the MAORY AO subsystem but are part of the E-ELT infrastructure. DetLGS, DetLO and DetRef size stand respectively for the size of the individual WFS-LGS, WFS-NGS-LO and WFS-NGS-Ref detectors

Fig. 2 shows an opto-mechanical representation of the MAORY instrument from the top. The LGS WFS is directly on the bottom of the MAORY bench (not visible in the figure).

2. THE LASER GUIDE STAR WAVEFRONT SENSOR

The LGS WFS will be located at the MAORY bench corner, below the MAORY bench, at an approximate altitude of 4 meters from the Nasmith platform (see Figure 3).

The objective will provide an optical beam with Focal ratio F/5, shorter than the focal ratio of the science focal plane in order to reduce the required focus range to track the sodium layer. The pupil will be seen by the LGS WFS at infinity distance in order to keep the exit pupil size constant for all sodium layer ranges. The sub-system will be not directly attached to the MAORY bench, but it will be interfaced through an interface plate that will also provide some regulation possibility for alignment procedures. The actual total weight of the system on the MAORY bench is around 800 kg.

In the following we give an overview of the sub-system in a schematic way, as a list of the main sub-system characteristics:

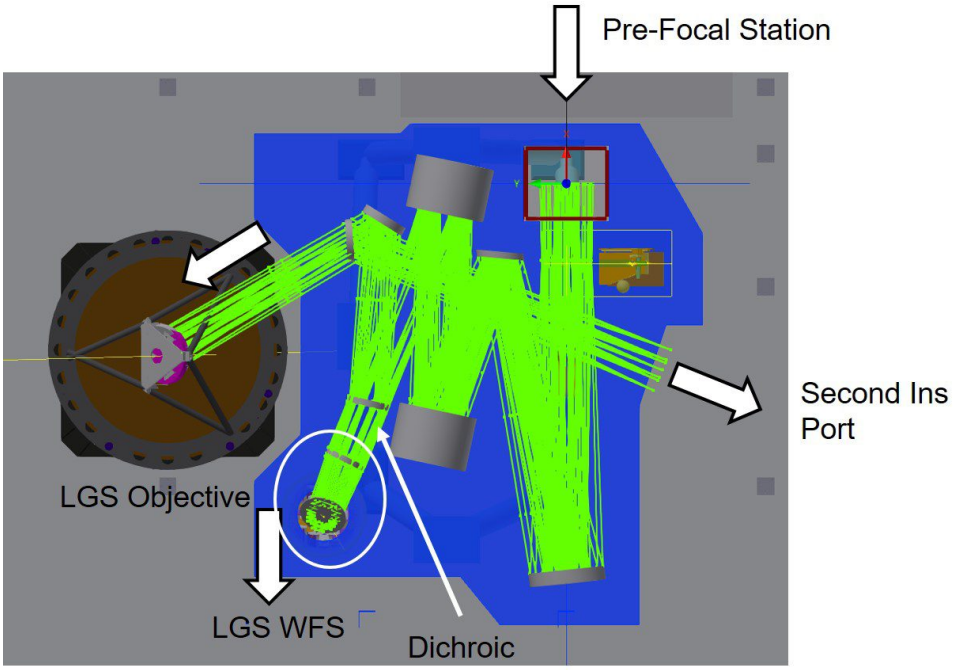

Figure 2. MAORY opto-mechanical overview: top view.

- It contains 6 high order Shack-Hartmann wavefront sensors disposed in an hexagonal geometry, mimicking the LGS constellation on sky. Each Shack-Hartmann is characterized 80×80 sub-apertures. In case of a phased ELT approach, the LGS WFS may also work with only four reference sources, even if the design will be optimized to work with six stars.
- It is gravity invariant.
- It is fixed with respect to the telescope pupil: this means that it is necessary to de-rotate with the telescope elevation.
- It must be able to compensate defocus: due to the varying elevation the distance of the Sodium Layer, the LGS with respect to the telescope pupil changes, hence the system must be able to keep the LGS spot 'in focus' in the sub-apertures. The required range goes up to infinity for calibration reasons during AIV phase at the telescope.
- The system should be able to go up to 700 frame per second (fps): the actual RTC requirement is anyway 500 fps.[4]
- It will be equipped with an internal calibration unit for Non Common Path Aberration (NCPA) calibration.

2.1 The LGS WFS key Technical specification: the Field of View

In this paragraph we illustrate some system aspects that have an important impacts on the LGS WFS sub-system specifications. These aspects helps to understand the rationale behind some key on-going trade-off study. In the era of the extremely large telescopes, in fact, we have to face some completely new challenges due to the telescope size itself. One of this peculiarities is the well known 'spot elongation effect'.[11,12] This comes from the combination of the non-negligible thickness of the Sodium layer and the laser launching position with respect to the pupil. When observing the LGS from a certain distance ($\geq 10m$), its shape is far from being a round spot. This is due to perspective elongation. In the case of ELT, with its almost 39 meters of diameter, the LGS would have in average a size of 10 arcseconds elongation if shot from the opposite side of the primary mirror, definitely

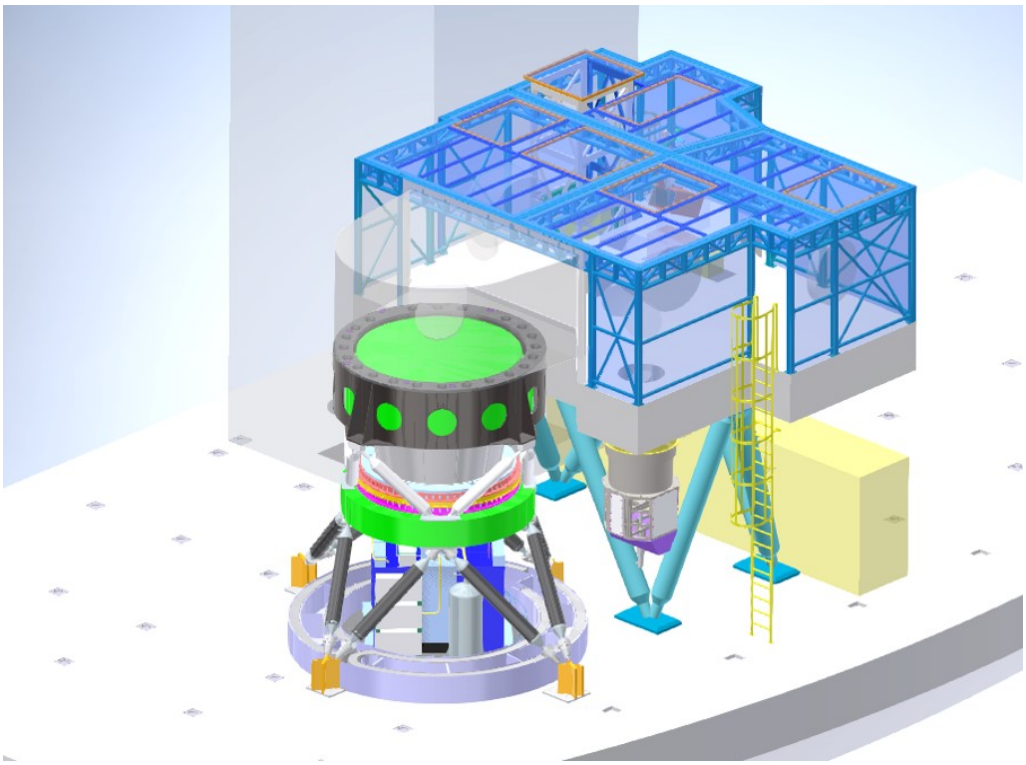

Figure 3. The LGS WFS position w.r.t. the MAORY bench.

larger then the seeing. It is apparent that this effect involves directly the LGS WFS, where the image of the LGS seen from different portions of the pupil is analyzed to compute the wavefront. The first immediate consequence of the elongation is the degradation of the slope measurements when using a Shack-Hartmann WFS. In the sub-apertures affected by elongation, the measurements could in fact result less precise due to a Signal reduction, because the source is no longer punctual but extended. Many papers in the literature has already faced this problem and it seems that a combination of smart centroiding, proper measurement weighting and information redundancy due to multiple stars should reduce the performance degradation.[13–15] Another interesting and critical aspect related to elongation is the sub-aperture Field of View (FoV) choice. The ideal situation would be to have a very large FoV in order to image the entire LGS spot in each sub-aperture, including those affected by elongation. Unfortunately this desiderable configuration is limited by technology: the available cameras for the MAORY LGS WFS, the LVSM CMOS mounted on the ESO camera LISA,[16] allows a maximum sub-aperture size of 10 pixels. As already mentioned, the elongated spot could reach 10-15 up to 20 arcseconds of elongation and, since the LGS image FWHM in the non elongated direction has been estimated around 1.5 arcseconds, more then 10 pixels are required to ensure enough FoV. In order to assign in an unambiguous way one spot to one sub-aperture, a field stop is therefore required to truncate the LGS spot wings in case of elongation. This cut could affect the centroid measurement in the truncated sub-apertures, causing the injection of spurious non-atmospheric medium order modes into the correction loop.[8] These modes are not static due to Sodium Layer density variation[17] and so they cannot be calibrated in an easy way. A truth wavefront sensor, the MAORY Reference wavefront sensor, will be able to see and measure these spurious aberrations during the observation. This wavefront sensor will have more than 10 sub-apertures to measure up to high orders and it will run in a range of 0.1-100 Hz depending on the Natural Guide Stars magnitude. Another way to face the problem, could be to increase the sub-aperture FoV by enlarging the pixel size. This implies also working with sub-sampled spots, a condition in which the WFS is not linear. After all, the sub-sampling of the spot could be faced by calibrating the centroid algorithm gain in real-time or, in case of large photon flux, slightly defocusing the laser. This long discussion was necessary to explain the actual MAORY choice to sub-sample the LGS spot with the

technical specification on sub-aperture FoV around 15 arcseconds. This specification has still to be confirmed by a trade-off study on going at ESO. The initial choice to work in a non linear regime only slightly affected by truncation effect was based on the fact that the truncation effect is still not well known and it could bring to unexpected surprises.

2.2 The LGS WFS Functionalities

In this section, we summarize the main functionalities of the LGS WFS sub-system.

- The WFS should be able to acquire two LGS constellations at 1.5 and 2 arcminutes diameter. A smooth transition between the two is not required during observation. The constellation diameter in the sky will remain constant during the observation, adjusting the Laser Facility launching angle. This will be managed by the interface between the MAORY RTC and the Telescope Central Control System.
- The WFS should de-rotate with telescope elevation for zenith angles between 1.5° to 70°.
- The WFS should be able to track in focus the sodium distance during observation. The WFS should also be able to focus at infinity distance. The focus correction should be spitted in two: a global focus regulation, common to all the WFS probes, and a focus regulation internal to each WFS probe, for the differential component.
- It should be also possible to align the pupil when required by the RTC (this functionality has still to be confirmed).

It is interesting to note that no LGS jitter correction functionality is internally foreseen. This correction will be done at the Laser Launching telescope level.

2.2.1 The Focus Correction

The LGS WFS will see a variable defocus term due to different contributions: atmospheric defocus, telescope elevation variation during observations, intrinsic sodium layer variations. The last two terms dominate. In the actual MAORY baseline, the atmospheric defocus is retrieved only from NGS measurements (Low order WFS). The LGS defocus is used to close a local secondary loop that keeps the LGS image close to focus. But how well the system should be in focus? This requirement should not be very critical until we are able to see a clear image of the LGS spots on the Shack-Hartmann. Anyway, a defocus signal causes also a shift in the LGS spots, and this shift could increase the already cited truncation effect. For this reason a maximum shift budget has been defined and this dominates the choices on the focus correction strategy. The total spot shift budged for dynamical errors is within 0.1 arseconds in all the sub-apertures and the absolute major contributor is indeed the defocus. The non-atmospheric defocus is made by two components: one predictable, due to telescope elevation changes, and another stochastic, due to intrinsic Sodium layer mean altitude variations. In order to define our strategy, we need to know also how often we need to apply the correction to satisfy the requirement. The two defocus components are characterized by different characteristic times, depending also on the zenith angle. For what concern the predictable component, we have computed the characteristic time considering the maximum zenith angle velocity of 13.64"/s. The non-predictable component has been derived by the PSD of the Sodium layer altitude variation. As reported in Ref. 17, the PSD of the Sodium layer altitude variation is expressed by the following equation:

$$P_a(\nu) = \alpha \nu^{\beta}, \tag{1}$$

where $\alpha = 31 m^2 HZ^{-1}$ and $\beta = -1.95$. The variation in altitude of the Sodium layer is directly related to a focus signal on the LGS WFS. At a certain zenith angle, we can define a variation in altitude that corresponds to a shift of the most elongated spot of 0.1 arcseconds in the sub-aperture. To compute the characteristic time we therefore compute the Sodium layer altitude structure function, that gives the characteristic average fluctuation on different time scales (see Fig. 4). As an example, when pointing at zenith, the altitude variation that would generate a shift of 0.1 arcseconds in the most elongated sub-aperture is around 84 m. From the curve reported in Fig. 4 we can see that this should happen about each 7 seconds.

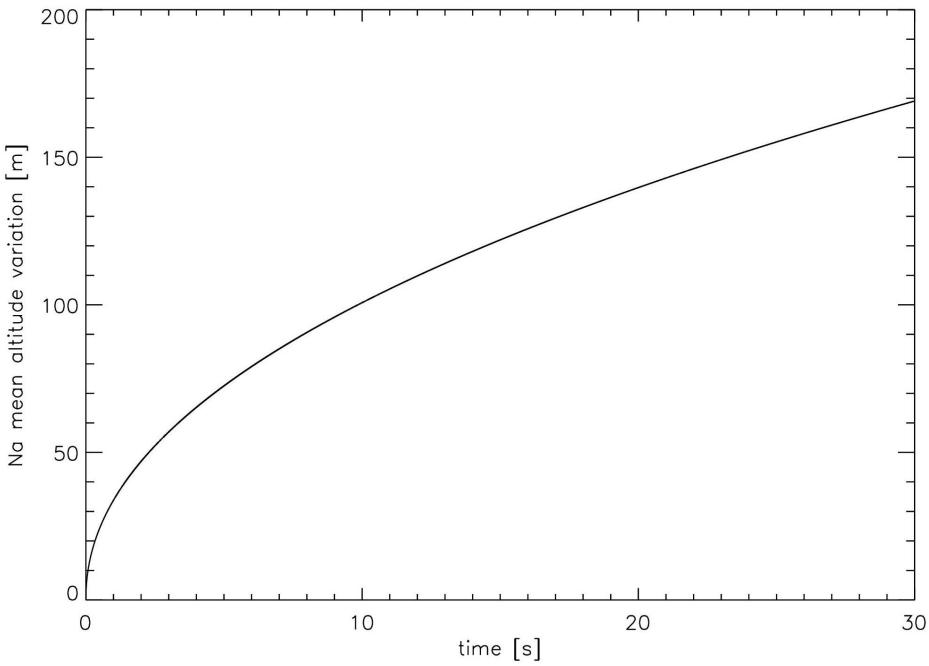

Figure 4. Sodium mean altitude variation as a function of time.

In Table 1 we report the time steps at each zenith angle that characterize a change in focus that corresponds to a spots shift of 0.1 arcseconds for both the components. Since the six LGS are slightly displaced one respect to the other to form the constellation in the sky, we can identify also a differential focus among the stars. This term and its variation is also reported in the table.

Table 1. Characteristic focus components variation time steps

Z change	1.5°	10°	30°	45°	70°
Predictable Common Focus (sec)	577	87	30.2	21.4	16.1
Stochastic Common Focus (sec)	6.8	7	9.2	14.2	67
Predictable Differential Focus (min)	0.38	3.23	10.6	18.3	50.4
Stochastic Differential Focus (min)	31.9	32.4	36.6	61.6	88.4

We would like to underline two interesting outcomes of Table 1. The first is that the non-predictable component dominates the common focus term; the second is that, if the average focus varies fast, the differential one seems to vary very slowly. Starting from this consideration, it is under evaluation the possibility to not correct for it in order to simplify the system.

Taking into account all the considerations reported above, two possible focus correction strategies are under study:

- To correct the common focus with a dedicated actuator, like a translation stage, and to leave to the internal focus only the responsibility to adjust for differential focus, if required. In this scenario, the translation stage would work almost all the time (in the worst case each 7 seconds) and the internal focus adjustment would occur with a very low frequency, unless we decide to completely remove this functionality;

- To use mainly the internal actuators, also to correct the common focus term, offloading to the common focus translation stage when close to the end of the internal focus dynamic range. For the internal focus we are thinking to use hexapods, one for each probe.

The final choice on the strategy will be based on many merit functions: actuators MTBF, actuators precisions, cooling power consumption, electrical power consumption and so on. As a first guess, the first scenario seems to be more interesting.

2.3 The LGS WFS Opto-mechanical design

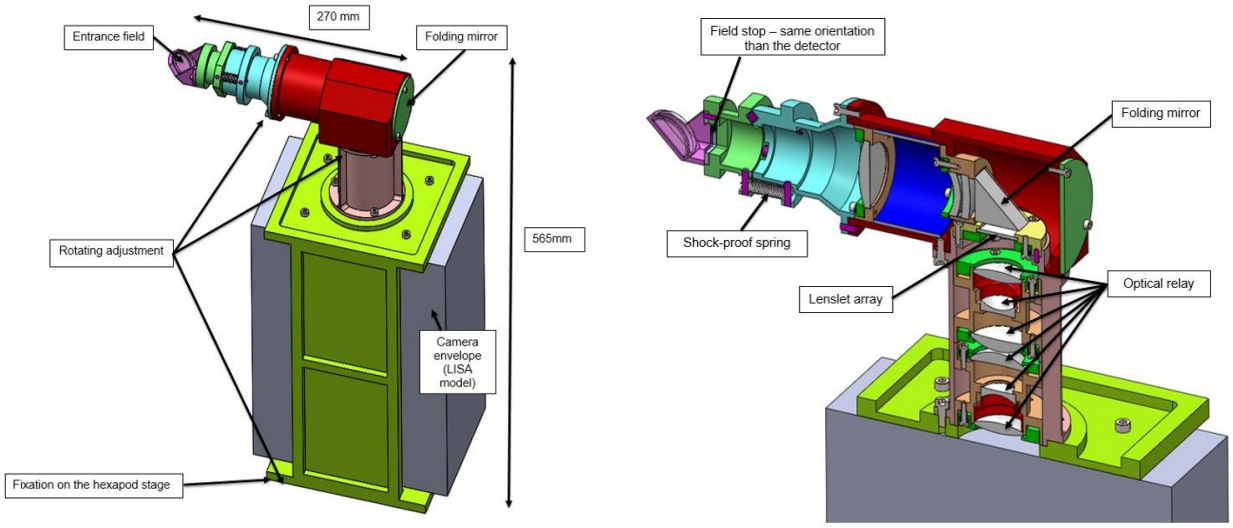

Figure 5. LGS WFS probe opto-mechanical design.

Fig. 5 represents the preliminary opto-mechanical design of one LGS WFS probe. The light coming from the LGS objective on the MAORY bench, is picked-up by a mirror at the entrance of the probe and then reflected downward in the direction of the LISA camera (represented as a big gray box in the Fig.). The 80×80 lenslet array is positioned just under the folding mirror and an optical relay re-image the LGS spots onto the camera detector. In the current design, the optical relay has a lenght of about $160mm$. The ESO camera LISA is represented as a volume, since no more details on the mechanics are given for the moment. The six probes will be identical with rotating adjustments to adapt for each LGS position.

Each LGS probe will be mounted on an hexapod actuator that assures many functionalities, like star acquisition, focus compensation and pupil alignment (Fig. 6). The six probes will be fixed on a common fixing plate in an hexagonal geometry, mimicking the LGS constellation. The pupil de-rotation will be carried out by a $700mm$ rotating stage. The six probes + rotation assembly will have a length of 835 mm.

The six probes assembly will be mounted on a common made-in-house sliding structure actuated by a stroke (Fig. 7 left side). The position is measured by an absolute scale on one of the rails on which the structure slides. Two cable ways allow 70° of rotation and $550mm$ of translation (to allow focusing at ∞). On the top of the the structure is mounted a completely retractable calibration unit for NCPA calibration (Fig. 7 right side).

The entire assembly will not be directly attached to the MAORY bench. An interface plate, with some adjustment possibility for alignment, is foreseen.

ACKNOWLEDGMENTS

The author thanks the Institut de Planétologie et d'Astrophysique de Grenoble (IPAG) for hospitality.

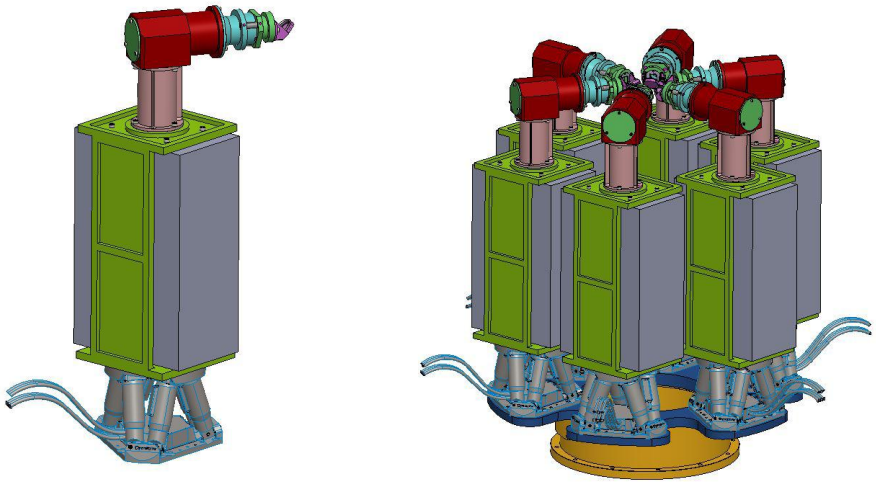

Figure 6. LGS WFS probes.

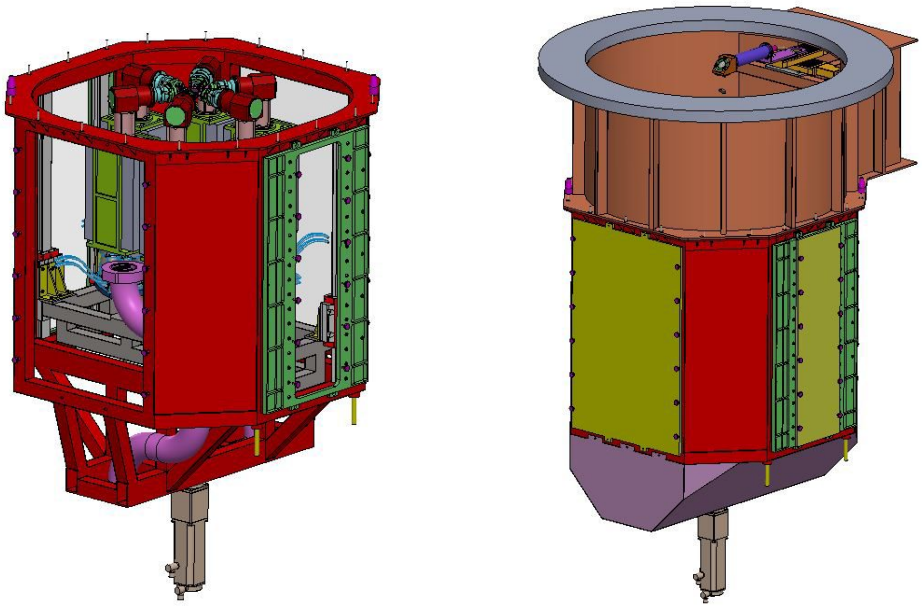

Figure 7. LGS WFS assembly.

REFERENCES

[1] Ciliegi, P. and others., "Maory for elt: preliminary design overview," in [*Adaptive Optics Systems VI*], *Proc. SPIE* **10703-38** (2018).

[2] Tamai, R. and others., "The eso's elt construction status," in [*Ground-based and Airborne Telescopes VII*], *Proc. SPIE* **10700**, 10700–36 (2018).

[3] Davies, R. and others., "The micado first light imager for elt: overview and operation," in [*Ground-based and Airborne Instrumentation for Astronomy VII*], *Proc. SPIE* **10702**, 10702–64 (2018).

[4] Foppiani, I. and others., "Maory real time computer preliminary design," in [*Adaptive Optics Systems VI*], *Proc. SPIE* **10703**, 10703–153 (2018).

[5] Bonaglia, M. and others., "Status of the preliminary design of the ngs wfs subsystem of maory," in [*Adaptive Optics Systems VI*], *Proc. SPIE* **10703**, 10703–164 (2018).

[6] Diolaiti, E. and Schreiber, L. and Foppiani, I. and Lombini, M. ., "Dual-channel multiple natural guide star wavefront sensor for the e-elt multiconjugate adaptive optics module," *Proc. SPIE* **8447**, 84471K (2012).

[7] Plantet, M. and others., "Performance analysis of the ngs wfs of maory," in [*Adaptive Optics Systems VI*], *Proc. SPIE* **10703**, 10703–156 (2018).

[8] Schreiber, L. and Diolaiti, E. and Arcidiacono, C. and Pfrommer, T. and Holzlöhner, R. and Lombini, M. and Hickson, P., "Impact of sodium layer variations on the performance of the e-elt mcao module," *Proc. SPIE* **9148**, 91486Q (2014).

[9] Bonnet, H. M. and others., "Adaptive optics at the eso elt," in [*Adaptive Optics Systems VI*], *Proc. SPIE* **10703**, 10703–37 (2018).

[10] Lombini, M. and others., "Optical design of the post focal relay of maory," in [*Ground-based and Airborne Instrumentation for Astronomy VII*], *Proc. SPIE* **10702**, 10702–355 (2018).

[11] Schreiber, L. and others., "Laser guide stars for extremely large telescopes: efficient shack–hartmann wavefront sensor design using the weighted centre-of-gravity algorithm," *Mon. Not. R. Astron. Soc.* **396**, 1513–1521 (2009).

[12] Robert, C., Conan, J.-M., Gratadour, D., Petit, C., and Fusco, T., "Shack-Hartmann tomographic wavefront reconstruction using LGS: analysis of spot elongation and fratricide effect," in [*Adaptative Optics for Extremely Large Telescopes*], 05010 (2010).

[13] Tallon, M., Tallon-Bosc, I., Béchet, C., Momey, F., Fradin, M., and Thiébaut, É., "Fractal iterative method for fast atmospheric tomography on extremely large telescopes," in [*Adaptive Optics Systems II*], *Proc. SPIE* **7736**, 77360X (July 2010).

[14] Neichel, B. et al., "The adaptive optics modes for HARMONI: from Classical to Laser Assisted Tomographic AO," in [*Adaptive Optics Systems V*], *Proc. SPIE* **9909**, 990909 (July 2016).

[15] Thomas, S., Fusco, T., Tokovinin, A., Nicolle, M., Michau, V., and Rousset, G., "Comparison of centroid computation algorithms in a Shack-Hartmann sensor," *Mon. Not. R. Astron. Soc.* **371**, 323–336 (Sept. 2006).

[16] Downing, M. and others., "Update on development of wfs cameras at eso for the elt," in [*Adaptive Optics Systems VI*], *Proc. SPIE* **10703**, 10703–69 (2018).

[17] Pfrommer, T. and Hickson, P., "Mesospheric sodium structure variability on horizontal scales relevant to laser guide star asterisms," *Proc. SPIE* **8447**, 844719 (2012).